Published in final edited form as:
Circ Arrhythm Electrophysiol. 2011 August 1; 4(4): 515–525. doi:10.1161/CIRCEP.111.962258.

Anatomic Localization and Autonomic Modulation of AV Junctional Rhythm in Failing Human Hearts

Vadim V. Fedorov, PhD[1], **Christina M. Ambrosi, MS**[1], **Geran Kostecki, BS**[1], **William J. Hucker, MD, PhD**[1], **Alexey V. Glukhov, PhD**[1], **Joseph P. Wuskell, PhD**[2], **Leslie M. Loew, PhD**[2], **Nader Moazami, MD**[3], and **Igor R. Efimov, PhD**[1]

[1]Department of Biomedical Engineering, Washington University in St. Louis, MO

[2]University of Connecticut Health Center, Farmington, CT

[3]Department of Surgery, Washington University School of Medicine, St. Louis, MO

Abstract

Background—The structure-function relationship in the atrioventricular junction (AVJ) of various animal species has been investigated in detail, however less is known about the human AVJ. In this study, we performed high-resolution optical mapping of the human AVJ (n=6) to define its pacemaker properties and response to autonomic stimulation.

Methods and Results—Isolated, coronary-perfused AVJ preparations from failing human hearts (n=6, 53±6 years) were optically mapped using the near-infrared, voltage-sensitive dye, di-4-ANBDQBS, with isoproterenol (Iso, 1 μM) and acetylcholine (ACh, 1μM). An algorithm detecting multiple components of optical action potentials was used to reconstruct multi-layered intramural AVJ activation and to identify specialized slow and fast conduction pathways (SP and FP). The anatomical origin and propagation of pacemaker activity was verified via histology. Spontaneous AVJ rhythms of 29±11 bpm (n=6) originated in the nodal-His region (NH, n=3) and/or the proximal His bundle (H, n=4). Iso accelerated the AVJ rhythm to 69±12 bpm (n=5); shifted the leading pacemaker to the transitional cell (TC) regions near the FP and SP (n=4) and/or coronary sinus (n=2); and triggered reentrant arrhythmias (n=2). ACh (n=4) decreased the AVJ rhythm to 18±4 bpm; slowed FP/SP conduction leading to block between the AVJ and atrium; and shifted the pacemaker to either the TC or TC/NH (bifocal activation).

Conclusions—We have demonstrated that the AVJ pacemaker in failing human hearts is located in the NH or H-regions and can be modified with autonomic stimulation. Moreover, we found that both the FP and SP are involved in anterograde and retrograde conduction.

Keywords

atrioventricular node; junctional rhythm; His bundle; optical mapping; heart failure

Introduction

The atrioventricular node (AVN), initially characterized by Sunao Tawara in 1906, describes a compact spindle-shaped network of cells connected to the His bundle.[1] Subsequent investigations have characterized two nodal extensions (rightward and leftward, RE and LE) extending proximally from the AVN towards the coronary sinus (CS).[2, 3] Consequently, the

Address for correspondence: Igor R. Efimov, Department of Biomedical Engineering, Washington University in St. Louis, Campus Box 1097, One Brookings Drive, St. Louis, MO 63130, Phone: (314) 935-8612, Fax: (314) 935-8377, igor@wustl.edu.

Conflict of Interest Disclosures: None.

term atrioventricular junction (AVJ) will be used in this study to describe all tissues involved in atrial-His conduction.[4]

Functionally, the AVJ plays an important role in maintaining AV conduction, functioning as a backup pacemaker in the setting of sinus node dysfunction, and protecting the ventricles during atrial tachyarrhythmias.[5–8] Microelectrode recordings from the rabbit AVJ have revealed several different cell types (transitional atrial-nodal [AN], compact nodal [N], and lower nodal-His [NH] regions) based on action potential morphology, which are functionally different from those recorded in typical atrial and His bundle cells.[9, 10] Moreover, cells of the AN, NH, and His regions of the AVJ exhibit independent pacemaker activity.[11] Additionally, the leading pacemaker and conduction properties of the AVJ are significantly modulated by the sympathetic and parasympathetic nervous systems.[5, 11–13]

Despite numerous detailed studies of the origin of excitation and conduction in the AVJ of many animal species,[11, 14, 15] only indirect measurements of the AVJ pacemaker have been reported in humans[5, 16–18] due to the inability of endocardial electrode mapping to determine the excitation origin and propagation of action potentials within the complex 3D structure of the AVJ.[15, 19, 20] Scherlag et al,[5] concluded that *"the nondescript, spurious nature of A-V nodal recordings would severely limit if not totally exclude their usefulness in differentiating the site of origin of junctional rhythms."* Moreover, the cellular electrophysiology of specific cell types in the AVJ region are likely driven by differential gene expression patterns for connexins and ion channels and are therefore not distinguishable by classical histological methods.[20, 21] A recent study by Greener et al,[22] however, has begun to unravel the complex, heterogeneous expression of genes in the AV conduction axis.

Optical mapping has made significant contributions to our understanding of conduction and pacemaker properties in the AVJ of various animal models.[13, 14, 23, 24] The more recent development of novel near-infrared voltage-sensitive fluorescent dyes allow for greater depth penetration and in-depth evaluation of the functional properties of complex structures, including the human sinoatrial node.[25, 26] In this study, we investigated pacemaker activity, conduction, and autonomic modulation of the human AVJ using high-resolution optical mapping with the voltage-sensitive dye, di-4-ANBDQBS with correlation of function to the underlying anatomical structures as defined via histology.

Methods

The use of human hearts for research was approved by the Institutional Review Board at Washington University in St. Louis.

In vitro optical mapping studies

Explanted failing human hearts (n=6, Figure 1A) were obtained at the time of cardiac transplantation (Barnes-Jewish Hospital, St. Louis, MO) and immediately arrested by cardioplegic solution (4°C), containing (in mM): 110 NaCl, 1.2 $CaCl_2$, 16 KCl, 16 $MgCl_2$, 10 $NaHCO_3$. Table 1 shows the clinical data regarding each specimen.

The AVJ was dissected from the whole heart and the posterior and/or anterior septal arteries were cannulated with 16-gauge catheters (Figure 1B). The final AVJ preparation included tissue of the interatrial and interventricular septa (IAS and IVS), central fibrous body (CFB), and coronary sinus (CS). The preparations were then positioned in a temperature-controlled glass chamber with the right septal endocardium facing the optical apparatus and superfused at 80 ml/min and coronary-perfused under a constant pressure of 55±5 mmHg with oxygenated (95% O_2, 5% CO_2) modified Tyrode's solution containing (in mM): 128.2

NaCl, 1.3 $CaCl_2$, 4.7 KCl, 1.05 $MgCl_2$, 1.19 NaH_2PO_4, 25 $NaHCO_3$, and 11 glucose. Temperature and pH were maintained continuously at 36±0.5°C and 7.35±0.05, respectively.

The excitation-contraction uncoupler blebbistatin[27] (10–20 μM, Tocris Biosciences, Ellisville, MO) and the voltage-sensitive dye, di-4-ANBDQBS[25] (10–40 μM) were added to the perfusate. Bipolar pacing and recording electrodes were placed at two locations on the IAS. Optical mapping was performed at a rate of 1000 frames/sec with the MiCam Ultima-L CMOS camera (SciMedia, Costa Mesa, CA) with an optical field of view (OFV) ranging from 28×28 to 33×33 mm^2 (280–330 μm/pixel).

Experimental protocol

After recording intrinsic AVJ rhythms under control conditions, the preparations were perfused with 1 μM Iso for 30 min, followed by 1 μM ACh for an additional 30 minutes. Our experimental protocol was limited to three hours based on our previous experience with optical mapping of the human sinoatrial node.[26]

Optical mapping data analysis and interpretations

Optical recordings contained fluorescent signals from the myocardium up to a depth of 1–3 mm.[23, 25, 28, 29] A custom-designed Matlab program was used to analyze multicomponent intramural optical action potentials (OAPs) as previously described.[30] Activation times and corresponding conduction velocities (CV) were defined in the nodal tissue and His bundle using 50% of the OAP amplitude (AP50%),[30, 31] while activation times of the atrial layer were defined by the dV/dt_{max} of the atrial upstroke component of the OAP.

Histology

After the optical mapping experiment, the AVJ preparations (n=5) were clearly marked with pins and frozen at −80°C. The tissues were cryosectioned at 16 μm and stained using Masson Trichrome (IMEB, San Marcos, CA). Anatomic structures of the His bundle, AV node, and nodal extensions were identified as described previously.[3]

3D model

The compartments of the AVJ were outlined in histological sections taken 250–500 μm apart throughout the entire length of the AVJ as follows: IAS/TC, IVS, connective tissue (valves and CFB), conduction system (His bundle, AVN, nodal extensions), and vasculature. The set of compartment outlines was then rendered to create a solid 3D volume in Rhinoceros NURBS modeling software (Robert McNeel and Associates, UK).

Statistics

Quantitative data are shown as mean±SD. The comparison of treatments was done using mixed model in PROC MIXED procedure of SAS 9.1 (Cary, NC). Post-hoc tests with Bonferroni adjustment were used to compare treatments.

Results

Anatomic Investigation of the Human AVJ

In order to precisely correlate function, as observed via optical mapping, with the underlying anatomical structures, five preparations were cryosectioned and histologically stained in order to verify the anatomical origin of OAPs as shown in Figure 1C. Rendering a volume based on individual anatomic structures into a 3D model, as shown in Figure 1D, allowed functional observations to be directly correlated to their anatomical structures.

Morphologically, we have divided the AVJ into the compact node (CN), two nodal extensions - rightward and leftward (RE and LE), and the proximal part of the His bundle.[2, 3] Individual histological sections, in addition to the 3D model, show that the entire AVN is encapsulated in fibrotic tissue, arteries, and fat from atrial and ventricular myocardial tissue layers except for the FP and SP areas, which morphologically represent the RE and LE.

Optical Mapping Aspects of Human AVJ during Atrial Pacing

Functionally, the AVJ was identified based on multicomponent OAPs corresponding to asynchronous activation of the atrial layers, AV nodal extensions, CN, and the His bundle as shown in Figure 2A during atrial pacing. In this example, OAP #5 is a purely atrial OAP, which is morphologically similar to a microelectrode recording. On the other hand, OAPs #1–4 contain at least two asynchronous components from AV nodal tissues, such as the rapidly rising upstroke of the atrial myocardium (Atrial component) located above the node and either the slowly rising upstroke of the AVN tissue (CN component) or rapidly rising upstroke of the His bundle (His component). As we have demonstrated earlier using simultaneous optical and microelectrode recordings,[23] these multiple components represent electrical activity in the near-surface atrial layer and the deeper structures of the AVN or His bundle.

By analyzing the rapidly rising and slowly rising upstrokes separately, we were able to map wavefront propagation through the various anatomical components separately as shown by the activation maps in Figure 2B. In this particular example of atrial pacing, the activation maps show that following an atrial stimulus, activation spread very quickly (CV up to 117 cm/sec) over the atrial tissue, entered both the FP and SP 35–40 ms after pacing, and then very slowly spread over the AVN (CV=2–6 cm/sec), reaching the His bundle in 230 ms with a final conduction velocity of up to 134 cm/sec.

Due to dissection of the distal His-Purkinje conduction system and/or diseased-associated conduction abnormalities, we did not observe intact AV conduction in any preparation. We did however, record transient conduction between the His bundle and IVS during Iso perfusion as shown in Online Figure 1.

Optical Mapping of the Human AVJ during Intrinsic Rhythm in Control

In addition to being paced, all preparations had spontaneous AVJ rhythms, an example of which is illustrated in Figure 3. The optical recordings with asynchronous components, as shown in Figure 3A, show different morphologies during spontaneous intrinsic activity, as compared to the OAPs recorded during atrial pacing in Figure 2A. In the example shown in Figure 3, OAPs #1–4, recorded from the AV node and proximal His bundle, exhibit rapidly rising upstrokes representative of the His bundle (His component), slowly rising upstrokes of the nodal tissues (AVN component), and rapidly rising upstrokes of the atrial myocardium (Atrial component). As shown in the activation maps in Figure 3B, spontaneous activation originated in the proximal part of the His bundle and rapidly spread along the bundle with retrograde CVs of up to 110 cm/sec. The retrograde excitation then slowly spread through the AVN, was blocked in the FP (or LE), but succeeded in spreading slowly and decrementally in the SP (or RE). Finally, excitation reached and activated the atrial myocardium near the classical SP ablation area. Subsequently, atrial activation led to anterograde re-excitation of the CN and His bundle via the FP.

During control junctional rhythms, the leading pacemaker was located in the proximal His bundle, such as shown in Figure 3. The remaining four preparations had leading pacemakers in the NH region as illustrated in Figure 4. In this second example of leading pacemaker

location, the recorded OAPs demonstrated variability in their sequence on a beat-to-beat basis due to weak conduction between the AVN and atrial myocardium, which led to complete exit block in 1 out of 8 beats (Figure 4Bc). This particular case of AVN exit block resulted in a pause of atrial activation and consequently provoked excitation of a competing intramural latent pacemaker in the TC region between the SP and CS (Figure 4Bd), which led to anterograde AVN activation (Figures 4Be and 4Bf). The clear presence of at least two conduction pathways (FP and SP) between the AVN and atrial myocardium were observed in all 6 preparations during intrinsic rhythm. Transient exit block of the impulse traveling from the AVN to the atrium, as is shown in Figure 4Bc, were observed in 3 of 6 preparations. In addition, intranodal longitudinal dissociation was observed in one preparation as shown in Online Figure 2.

Effects of Acetylcholine and Isoproterenol on AVJ Automaticity and Conduction

After detecting the location of the leading pacemaker under control conditions, we perfused the preparations with 1 μM Iso (n=5), followed by 1 μM ACh (n=4). Figure 5 shows a representative example of OAPs and conduction patterns recorded during stable junctional rhythm in control conditions (Figure 5A), after Iso (Figure 5B), and after ACh (Figure 5C). Under control conditions, intrinsic excitation originated in the proximal part of the His bundle, spread via the His bundle and compact AVN over 35 ms, slowly propagated through the FP, and decrementally spread through the SP. At 80 ms atrial myocardium was activated through the FP (atrial breakthrough) at the site indicated by a white ellipse in the atrial map of Figure 5A. Application of 1μM Iso in this preparation resulted in rhythm acceleration to 81 BPM and anatomical shift of the AVJ leading pacemaker to the CN region as shown in the corresponding AVN map of Figure 5B. Under these conditions, excitation reached atrial myocardium simultaneously and rapidly (30 ms) through both the FP and SP located 14 mm apart. Finally, application of 1 μM ACh resulted in complete depression of all pacemaker activity in the AVJ for 2 minutes, followed by 3 minutes of gradual recovery of the intrinsic activity with the leading pacemaker in the TC areas near SP and FP. As shown in Figure 5C, atrial activation had two breakthroughs due to intramural conduction from the TC pacemaker. This activation entered the AVN through both the FP and SP, however, the excitation wave propagated faster through the FP thus exciting the CN first at 90 ms and very quickly propagating through the His bundle, while the SP wave propagated more slowly. Figures 5D and E show the anatomical locations of the leading pacemakers, confirming our functional observations of the complex intramural conduction of this preparation.

Additionally in this preparation, washout of ACh led to recovery of the proximal His pacemaker (as in control, Figure 5A) and competition of two pacemakers was observed as illustrated in Online Figure 3. We observed this pacemaker shift and subsequent competition of multiple pacemakers during perfusion of Iso and during washout of ACh in all AVJs studied. However, in contrast to some preparations, in which Iso (Online Figure 1) or ACh (Figure 5B) induced an anatomic shift of the main pacemaker out of the AVN, the leading pacemaker of AVJ #5 remained at the same location in the NH region during approximately 80% of recorded beats, while presenting dramatic rhythm changes from 76 BPM (Iso) to 18 BPM (ACh) (Online Figure 4).

Perfusion with Iso also induced nonsustained reentrant arrhythmias (2–5 beats) in 3 out of 5 preparations. Figure 6 shows an example of a nonsustained (4 beat) reentrant arrhythmia, induced due to acceleration of AVN pacemaker activity and functional longitudinal dissociation in AVJ #2 (see also Online Figure 2).

In summary, Figure 7A shows the sites of all pacemakers detected in all seven preparations under all conditions. The sites were widely distributed, primarily within the AVJ, but

occasionally were also found outside of the AVJ within the atrial myocardium. On average, Iso significantly accelerated the AVJ rhythm from 29±11 up to 69±12 BPM ($p<0.001$) as shown in Figure 7B, whereas ACh significantly decelerated AVJ rhythms to 18±4 BPM ($p<0.001$).

Discussion

Structural and functional characteristics of the human AVJ

This study used optical mapping to show the location of the leading pacemaker and conduction patterns within the AVJ during autonomic stimulation in isolated human preparations for the first time. The human AVJ is a complex 3D structure that is anatomically and functionally isolated from the atrial and ventricular myocardium except for several conduction pathways as illustrated anatomically in Figure 1. Without autonomic stimulation in these denervated AVJs, intrinsic excitation originated in NH or H regions, then slowly propagated from the AVN via the FP and/or SP to the atrial myocardium. Thus, atrial breakthrough sites (exit points from the conduction pathways) could be located 7 to 21 mm from the leading pacemaker site. Beta-adrenergic stimulation by Iso and cholinergic stimulation by ACh produced pacemaker shifts within or outside of the AVN as summarized in Figure 7. Our observations in this study support the clinical observation of the existence of multiple pacemakers in the AVJ and their sensitivities to adrenergic and cholinergic agents.[5, 8, 18] Clinically, conduction in the AVJ is often thought of in terms of fast and slow pathway conduction. Conduction velocity is a function of both the ionic currents that create the action potential as well as the connexin proteins which compose the electrical synapses (gap junctions) between myocytes. Our recent functional[31] and anatomic[3] studies have demonstrated that there are two anatomic compartments of the AVJ defined by the presence or absence of Cx43. Based on the data of the current study and our prior results, we conclude that fast pathway conduction involves a layer of transitional cells which communicate with a Cx43-negative continuous structure composed of the leftward INE, CN, and a Cx43-negative compartment of the His bundle. Anatomically, these structures that participate in FP conduction are located along the superior border of the triangle of Koch. Slow pathway conduction involves a layer of transitional cells that communicates with a continuous Cx43 positive structure composed of the rightward INE, the lower nodal bundle of the CN, and a Cx43 positive compartment of the His bundle. This conduction pathway is located along the inferior border of the triangle of Koch, along the tricuspid annulus. Similarly, a recent study by Greener et al[22] carefully investigated mRNA levels throughout the AVJ and found that the expression profile of tissues involved in fast pathway conduction were more likely to support fast conduction with higher levels of $Na_V1.5$, Cx40, and low Cx43 whereas less $Na_V1.5$ was expressed in the rightward INE. In that study, similar expression levels of Cx43 were found between the rightward INE and the CN, however that study did not divide the lower nodal bundle from the CN itself. Therefore a growing body of evidence from multiple modalities (mRNA and protein expression assays, immunohistochemistry, optical mapping) supports the idea that the dual pathway physiology well known to exist in the AVJ is a consequence of compartmentalized protein expression patterns throughout the AVJ. These expression patterns result in longitudinal dissociation of conduction within the AVJ with faster conduction in the superior aspect of the AVJ and slower conduction in the inferior portion of the AVJ. These differential conduction properties provide the fundamental substrate necessary for AVNRT.

Interestingly, we found previously that unlike the rabbit SAN pacemaker[32] which shifts in response to autonomic stimulation, the rabbit AVJ pacemaker remains stationary (most often in the SP).[13] Contrary to those results, this study showed that in the denervated human AVJ rhythms originate in the NH/H region in the absence of autonomic tone or stimulation. This is the first demonstration of the location of the junctional pacemaker by optical mapping in

the human. Clinically the rate of the junctional pacemaker is thought to be slower further down in the AVJ, i.e a high junctional pacemaker has a higher rate than a pacemaker located in the His bundle. In this study, the average rate of denervated AVJ was 29±11 bpm (which is slower than a typical junctional rhythm clinically) and originated in the NH-His region of the AVJ. Therefore the slow rate of the AVJ pacemaker seen in this study is consistent with its origin near the His bundle, and it is possible that a junctional rhythm at a higher rate may be seen in future studies originating more proximally in the AVJ. As mentioned in the study limitations, there are many factors that may have influenced the junctional rate in these preparations including inotropic therapy, long term pacing, β-blocker therapy, and denervation, so future studies in normal hearts will need to be pursued to investigate the AVJ pacemaker under more normal circumstances.

Specific features of the optical mapping of the human AVJ

The present study extends our methodological approaches, introduced earlier in rabbit[23] canine,[30] and human[31] studies, allowing for structure/function mapping of the SAN and AVN in large mammalian species, possibly due to improvements in signal processing, enhanced resolution of optical mapping afforded by the Ultima-L CMOS camera (SciMedia, Costa Mesa, CA), and the development of novel near-infrared voltage-sensitive dyes, such as di-4-ANBDQBS. Consequently, we were able to detect optical signals in all or most of the deeper structures of the human AVJ and track conduction through it without “blind” time windows. This is in contrast to our previous study of the human AVJ with di-4-ANEPPS, which yielded optical signals only from sub-endocardial structures of the His bundle regions, but failed to document electrical activity in the nodal extensions.[31]

Thus, the combination of optical mapping and histology have allowed us to demonstrate His bundle and AVN intramural activation patterns, track conduction pathways such as the FP and SP, and pinpoint sites of atrial breakthroughs. As was shown in Figure 4, multicomponent OAPs occurred not only in the structural AVJ region, but also in TC regions near the nodal extensions due to the presence of multiple conduction and/or intramural pacemaker tissue layers. Another important contribution of our study is that our data provides fundamental data such as conduction velocities to guide the ongoing development to mathematical models of AVJ conduction.

Study limitations

It goes without saying that explanted failing hearts are not physiologically normal. As cardiac transplantation is a treatment of last resort, these hearts have been subjected to multitudes of therapeutic interventions, including long term β-blocker therapy, ACE inhibition, digoxin, long term pacing, LVAD (heart #3), and inotropic support for an unknown duration (hearts # 4 and 6). The influence of these interventions on AV conduction, response to isoproterenol and acetylcholine, and on pacemaking in the AV junction is not known. Similarly 5 of 6 hearts in this study had an AICD (one with a BiV AICD) and the effect of pacing from the AICD is not known. Our knowledge of the clinical course of these patients prior to transplant is very limited, and therefore we do not know their level of conduction system disease or how pacer-dependent they were prior to transplant, and these factors could clearly influence the results of our study. It is also possible that long-term β-blocker therapy and inotrope use may have altered the AVJ response to autonomic agents in our study. To decipher the influence of these factors, future studies will have to include normal AVJs that were rejected from transplant. Finally it is important to note that the hearts in this in vitro study were denervated.

Experimentally, we cannot exclude the potential influence of ischemia and edema that may develop in a mechanically silent preparation and consequently may affect AVJ pacemaker

and conduction properties. To mitigate these effects, the duration of our optical mapping experiments was limited to three hours.[26] Finally, even new, long-wavelength infrared dyes cannot guarantee complete penetration into the entire 3D structure of the AVJ. As with signals generated by electrical potentials, interpretation of OAPs require an understanding of the multiple, distinct sources from various tissue layers that contribute to signal morphology. Consequently, a complex signal characterization and correlation with appropriate anatomical sources must be undertaken.[29]

Conclusions

In conclusion, we found that, under control conditions, the leading pacemaker of the human AVJ is located in the NH and H regions. Its rhythm can be modulated by autonomic stimulation, through the application of Iso and ACh, resulting in rhythms ranging from 13 to 81 BPM. We found that the main conduction delay occurs in the AVJ inputs, namely the SP and FP, but not in the AVN itself whose conduction is modulated by autonomic stimulation. In all hearts, both the FP and SP are involved in anterograde and retrograde conduction with multiple connections existing between the FP, SP, and atrial myocardium, as evident from multiple retrograde atrial exit sites in addition to observed reentrant activity. Consequently, dual AVN physiology should be considered a normal finding in the human heart and additional factors, such as distinct molecular expressions patterns, may be required for clinical AV nodal reentrant tachycardia (AVNRT) to manifest. Finally, longitudinal dissociation is evident between nodal extensions, which exhibit simultaneous multiple pacemaker activity that could in part be responsible for AVNRT.

Supplementary Material

Refer to Web version on PubMed Central for supplementary material.

Acknowledgments

The authors thank Dr. Stanislav Zakharkin for help in statistical analysis of the data.

Funding Sources: NIH grant R01 HL085369

References

1. Tawara, S. Das Reizleitungssystem des Saugetierherzens: Eine Anatomisch-Histologische Studie Uber Das Atrioventrikularbundel Und Die Purkinjeschen Faden. Jena: Verlag von Gustav Fischer; 1906.
2. Inoue S, Becker AE. Posterior extensions of the human compact atrioventricular node: a neglected anatomic feature of potential clinical significance. Circulation. 1998; 97:188–193. [PubMed: 9445172]
3. Hucker WJ, McCain ML, Laughner JI, Iaizzo PA, Efimov IR. Connexin 43 expression delineates two discrete pathways in the human atrioventricular junction. Anat Rec (Hoboken). 2008; 291:204–215. [PubMed: 18085635]
4. Billette J. What is the atrioventricular node? Some clues in sorting out its structure-function relationship. J Cardiovasc Electrophysiol. 2002; 13:515–518. [PubMed: 12030537]
5. Scherlag BJ, Lazzara R, Helfant RH. Differentiation of “A-V junctional rhythms”. Circulation. 1973; 48:304–312. [PubMed: 4726210]
6. Hoffman, BF.; Cranefield, PF. Electrophysiology of the Heart. New York: McGraw-Hill; 1960.
7. de Azevodo IM, Watanabe Y, Dreifus LS. Atrioventricular junctional rhythm: classification and clinical significance. Chest. 1973; 64:732–740. [PubMed: 4128193]
8. Alison JF, Yeung-Lai-Wah JA, Schulzer M, Kerr CR. Characterization of junctional rhythm after atrioventricular node ablation. Circulation. 1995; 91:84–90. [PubMed: 7805223]

9. de Carvalho AP, de Almeida DF. Spread of activity through the atrioventricular node. Circ Res. 1960; 8:801–809. [PubMed: 13808074]
10. Billette J. Atrioventricular nodal activation during periodic premature stimulation of the atrium. Am J Physiol. 1987; 252:H163–177. [PubMed: 3812708]
11. Watanabe Y, Dreifus LS. Sites of impulse formation within the atrioventricular junction of the rabbit. Circ Res. 1968; 22:717–727. [PubMed: 4298205]
12. Chiou CW, Eble JN, Zipes DP. Efferent vagal innervation of the canine atria and sinus and atrioventricular nodes. The third fat pad. Circulation. 1997; 95:2573–2584. [PubMed: 9184589]
13. Hucker WJ, Nikolski VP, Efimov IR. Autonomic control and innervation of the atrioventricular junctional pacemaker. Heart Rhythm. 2007; 4:1326–1335. [PubMed: 17905339]
14. Dobrzynski H, Nikolski VP, Sambelashvili AT, Greener ID, Yamamoto M, Boyett MR, Efimov IR. Site of origin and molecular substrate of atrioventricular junctional rhythm in the rabbit heart. Circ Res. 2003; 93:1102–1110. [PubMed: 14563715]
15. de Bakker JM, Loh P, Hocini M, Thibault B, Janse MJ. Double component action potentials in the posterior approach to the atrioventricular node: do they reflect activation delay in the slow pathway? J Am Coll Cardiol. 1999; 34:570–577. [PubMed: 10440175]
16. McGuire MA, Bourke JP, Robotin MC, Johnson DC, Meldrum-Hanna W, Nunn GR, Uther JB, Ross DL. High resolution mapping of Koch's triangle using sixty electrodes in humans with atrioventricular junctional (AV nodal) reentrant tachycardia. Circulation. 1993; 88:2315–2328. [PubMed: 8222125]
17. Yu JC, Lauer MR, Young C, Liem LB, Hou C, Sung RJ. Localization of the origin of the atrioventricular junctional rhythm induced during selective ablation of slow-pathway conduction in patients with atrioventricular node reentrant tachycardia. Am Heart J. 1996; 131:937–946. [PubMed: 8615313]
18. Shepard RK, Natale A, Stambler BS, Wood MA, Gilligan DM, Ellenbogen KA. Physiology of the escape rhythm after radiofrequency atrioventricular junctional ablation. Pacing Clin Electrophysiol. 1998; 21:1085–1092. [PubMed: 9604240]
19. Hoffman BF, Cranefield PF, Stuckey JH, Bagdonas AA. Electrical activity during the P-R interval. Circ Res. 1960; 8:1200–1211. [PubMed: 13715001]
20. McGuire MA, de Bakker JM, Vermeulen JT, Moorman AF, Loh P, Thibault B, Vermeulen JL, Becker AE, Janse MJ. Atrioventricular junctional tissue. Discrepancy between histological and electrophysiological characteristics. Circulation. 1996; 94:571–577. [PubMed: 8759104]
21. Meijler FL, Janse MJ. Morphology and electrophysiology of the mammalian atrioventricular node. Physiol Rev. 1988; 68:608–647. [PubMed: 2451833]
22. Greener ID, Monfredi O, Inada S, Chandler NJ, Tellez JO, Atkinson A, Taube M-A, Billeter R, Anderson RH, Efimov IR, Molenaar P, Sigg DC, Sharma V, Boyett MR, Dobrzynski H. Molecular architecture of the human specialized atrioventricular conduction axis. J Mol Cell Cardiol. 2011; 50:642–51. [PubMed: 21256850]
23. Efimov IR, Mazgalev TN. High-resolution, three-dimensional fluorescent imaging reveals multilayer conduction pattern in the atrioventricular node. Circulation. 1998; 98:54–57. [PubMed: 9665060]
24. Wu J, Olgin J, Miller JM, Zipes DP. Mechanisms underlying the reentrant circuit of atrioventricular nodal reentrant tachycardia in isolated canine atrioventricular nodal preparation using optical mapping. Circ Res. 2001; 88:1189–1195. [PubMed: 11397786]
25. Matiukas A, Mitrea BG, Qin M, Pertsov AM, Shvedko AG, Warren MD, Zaitsev AV, Wuskell JP, Wei MD, Watras J, Loew LM. Near-infrared voltage-sensitive fluorescent dyes optimized for optical mapping in blood-perfused myocardium. Heart Rhythm. 2007; 4:1441–1451. [PubMed: 17954405]
26. Fedorov VV, Glukhov AV, Chang R, Kostecki G, Aferol H, Hucker WJ, Wuskell JP, Loew LM, Schuessler RB, Moazami N, Efimov IR. Optical mapping of the isolated coronary-perfused human sinus node. J Am Coll Cardiol. 2010; 56:1386–1394. [PubMed: 20946995]
27. Fedorov VV, Lozinsky IT, Sosunov EA, Anyukhovsky EP, Rosen MR, Balke CW, Efimov IR. Application of blebbistatin as an excitation-contraction uncoupler for electrophysiologic study of rat and rabbit hearts. Heart Rhythm. 2007; 4:619–626. [PubMed: 17467631]

28. Nikolski V, Efimov I. Fluorescent imaging of a dual-pathway atrioventricular-nodal conduction system. Circ Res. 2001; 88:E23–30. [PubMed: 11179207]

29. Efimov IR, Fedorov VV, Joung B, Lin SF. Mapping cardiac pacemaker circuits: methodological puzzles of the sinoatrial node optical mapping. Circ Res. 2010; 106:255–271. [PubMed: 20133911]

30. Fedorov VV, Schuessler RB, Hemphill M, Ambrosi CM, Chang R, Voloshina AS, Brown K, Hucker WJ, Efimov IR. Structural and functional evidence for discrete exit pathways that connect the canine sinoatrial node and atria. Circ Res. 2009; 104:915–923. [PubMed: 19246679]

31. Hucker WJ, Fedorov VV, Foyil KV, Moazami N, Efimov IR. Images in cardiovascular medicine. Optical mapping of the human atrioventricular junction. Circulation. 2008; 117:1474–1477. [PubMed: 18347223]

32. Fedorov VV, Hucker WJ, Dobrzynski H, Rosenshtraukh LV, Efimov IR. Postganglionic nerve stimulation induces temporal inhibition of excitability in rabbit sinoatrial node. Am J Physiol Heart Circ Physiol. 2006; 291:H612–623. [PubMed: 16565321]

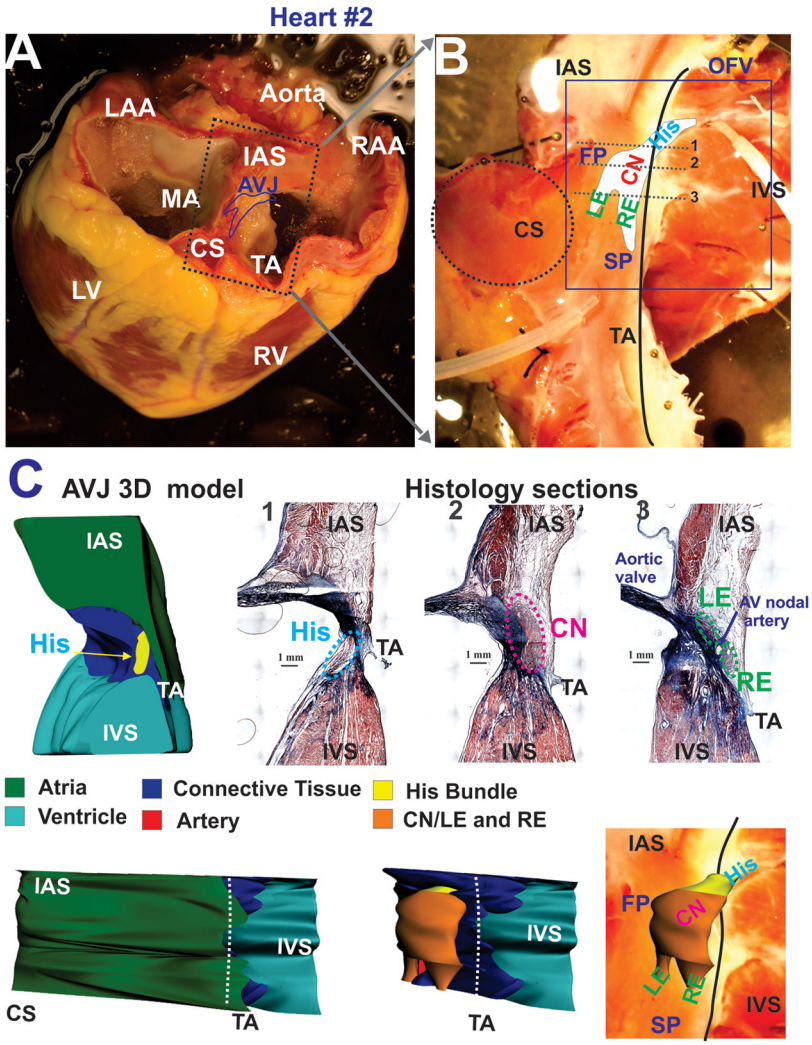

Figure 1.

Explanted heart #2 and anatomy of the experimental preparation. **Panel A**: A photograph of explanted failing human heart #2 before dissection. The approximate borders of the AV junction (AVJ) are shown by the dark blue line. Abbreviations: RV and LV: right and left ventricles; MA and TA: mitral and tricuspid valve annulus; RAA and LAA: right and left atrial appendages; IAS: interatrial septa, CS: coronary sinus. **Panel B:** A photograph of the coronary-perfused human AVJ preparation with an optical field of view (OFV) which included: compact node (CN), leftward (LE) and rightward extensions (RE), and the bundle of His (His). Gray dotted lines show the location of histological sections illustrated in panel C. Abbreviations: SP and FP: slow and fast pathways; IVS: intraventricular septa. **Panel C:** Histology sections through the NH region (His), compact AV node (CN), and extensions (RE and LE) from sites 1–3 in panel B. **Panel D:** 3D anatomical reconstruction of AVJ #2 from histological sections. Top - Cross-section in projection zx, which corresponds to histology slide 1 in panel C. Middle and Bottom –endocardial projection (xy) of the AVJ with and without the atrial myocardial layer displayed.

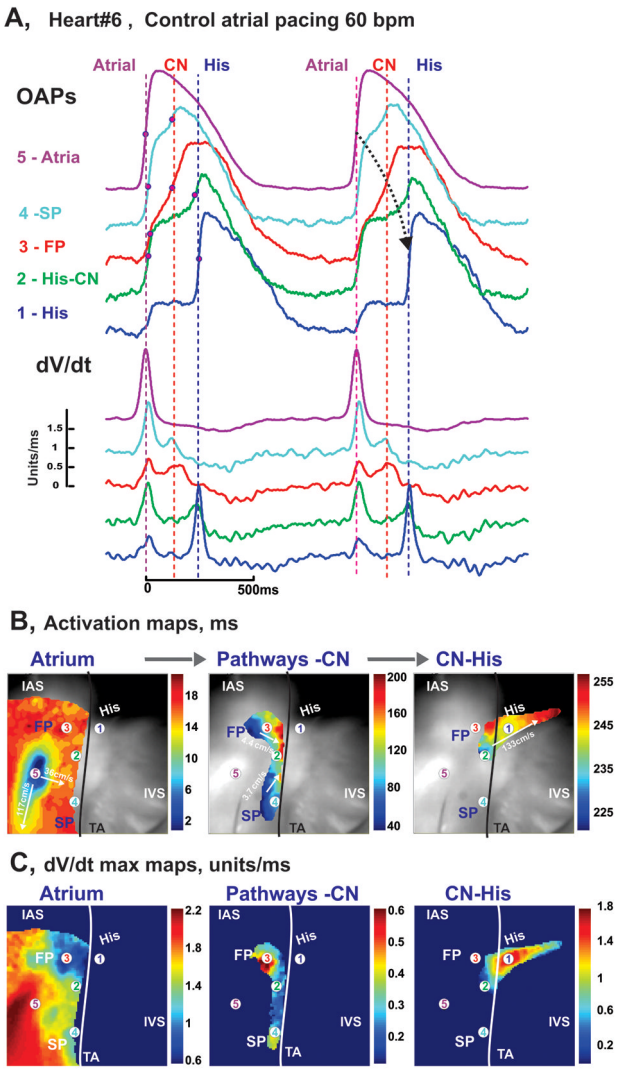

Figure 2.

Optical mapping of AVJ #6 during atrial pacing. **Panel A:** OAPs and their derivatives recorded from sites 1–5 in panels B and C, during atrial pacing at 60 bpm (CL=1000ms). Red dots on OAP upstrokes correspond to dV/dt peaks. **Panel B:** Separated atrial, AV nodal, and His bundle activation maps superimposed on the OFV (30×30 mm^2). The black line demarcates the TA.

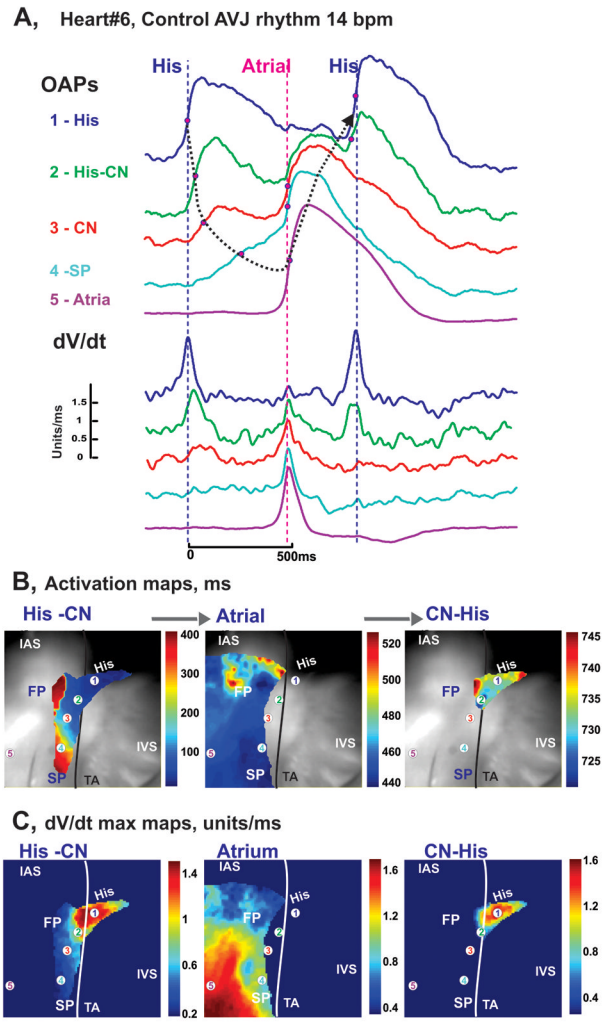

Figure 3.

Optical mapping of AVJ #6 during intrinsic rhythm. **Panel A:** OAPs and their derivatives recorded from sites 1–5 in panel B during spontaneous AVJ rhythm (12 bpm). **Panel B:** Separated His-AVN, atrial, and His activation maps superimposed on the OFV (30×30 mm^2).

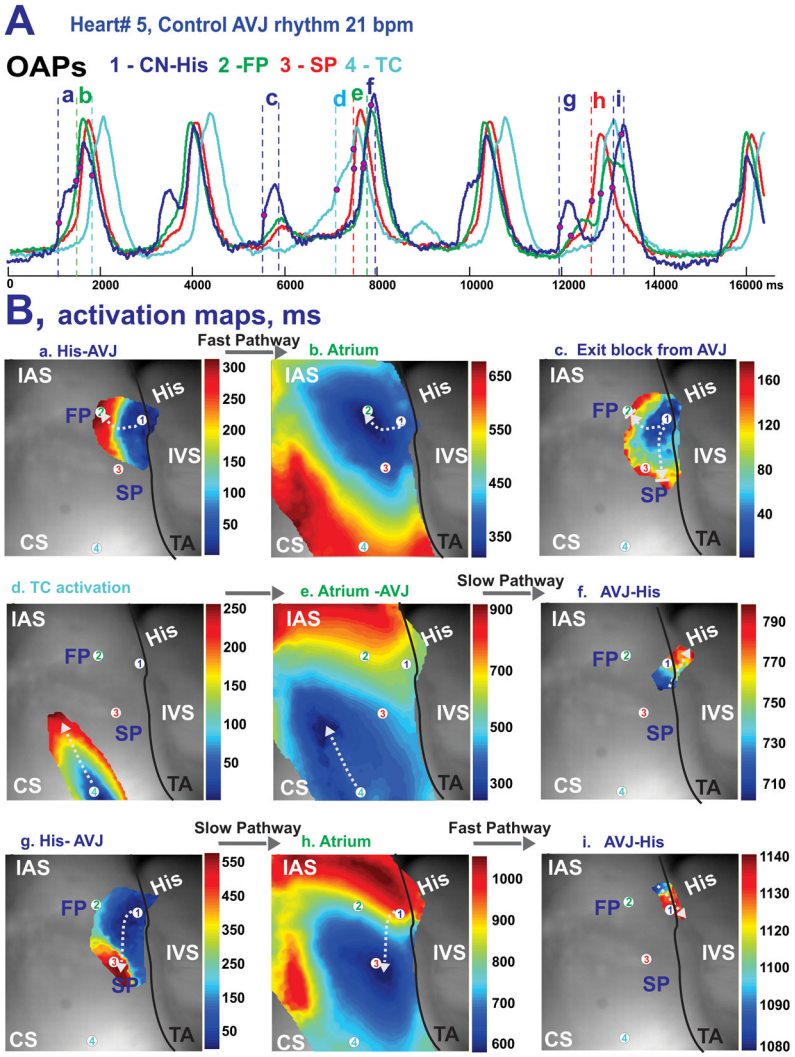

Figure 4.

Optical mapping of AVJ #5 during intrinsic rhythm under control conditions. **Panel A:** OAPs from the NH region (CN-His), fast and slow conduction pathways (FP and SP), and TC region near the CS recorded from sites #1–4 in panel B during intrinsic AVJ rhythm. **Panel B:** Activation maps of the different tissue layers during: FP conduction between AV node (a) and atria (b); exit block from the AV node (c); shift of the leading pacemaker to the TC region (d) followed by activation of atrial and AVJ tissues (e and f); and during SP conduction between AV node (f) and atria (h), and then AVJ again (i). The white arrows indicate the wave propagation directions from the different tissue layers.

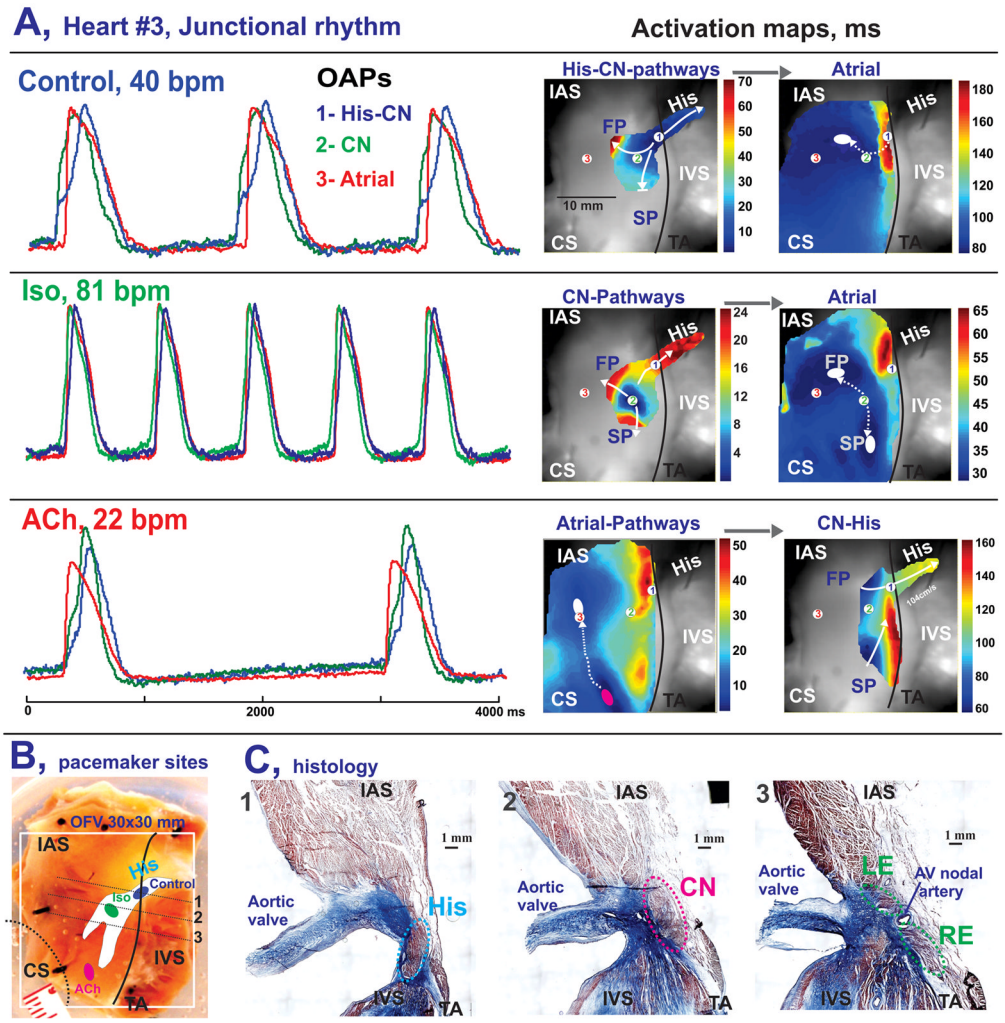

Figure 5.

Optical mapping of AVJ #3 during autonomic stimulation. **Panels A–C:** OAPs and activation maps of the different tissue layers during spontaneous AVJ rhythm in control (A), after a 10 minute perfusion of Iso (B), and after a 10 minute perfusion with ACh (C). OAPs were recorded from the NH region (1-His-CN, blue), compact node (2-CN, green) and interatrial septum (3-Atria, red). The white ovals show atrial breakthrough sites as recorded by optical mapping. Pink oval shows leading pacemaker site during ACh perfusion. **Panel D:** A photograph of the AVJ preparation before histology dissection procedure. Colored ovals show location of the leading pacemaker sites obtained from panels A-C. **Panel C:** Histology sections through the NH region (His), compact AV node (CN), and leftward (LE) and rightward extensions (RE), as indicated by the dotted gray line in panel D, show the anatomical locations of the main AVJ pacemakers.

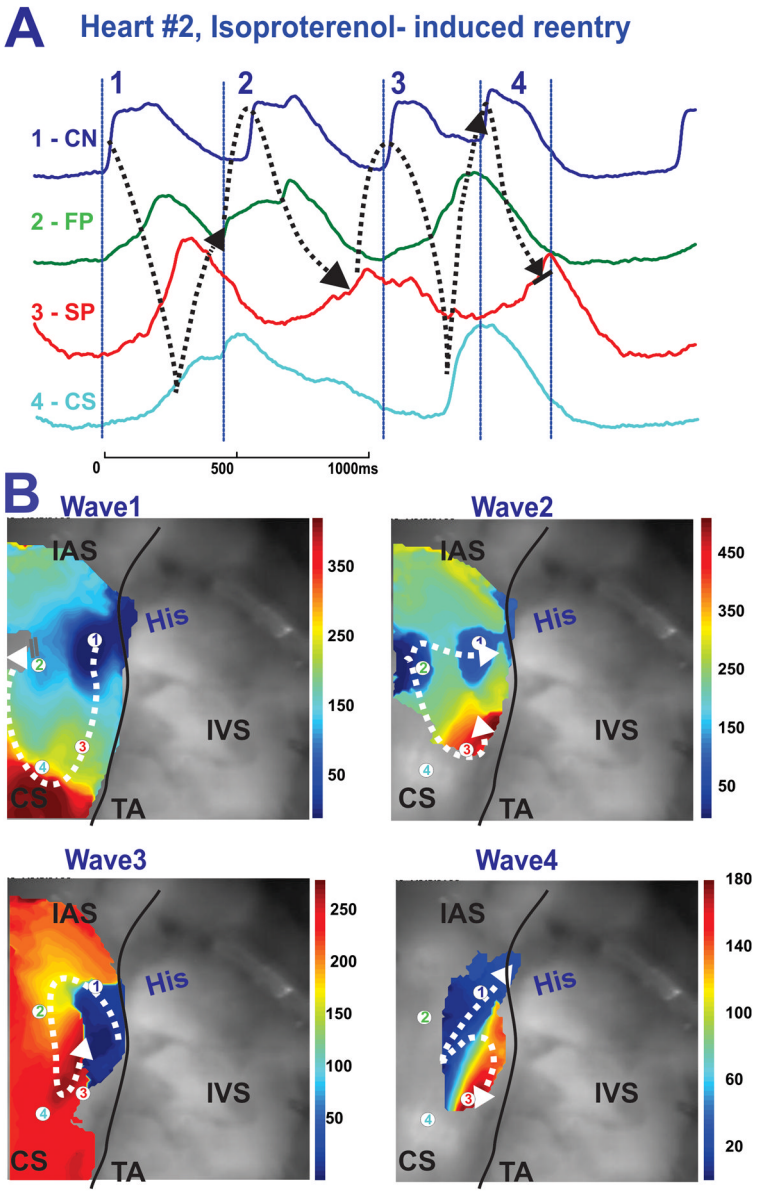

Figure 6.

Reentrant activity induced by Isoproterenol. **Panel A:** OAPs from the CN region (CN-His), fast and slow conduction pathways regions (FP and SP), and TC region near the CS recorded from sites 1–4 as indicated on the activation maps in panel B during spontaneous reentrant activity in the AVJ. The black dotted arrows show the propagation of reentrant activity **Panel B:** Activation maps showing the complex reentrant circuits during reentrant activity. The white arrows show the directions of conduction.

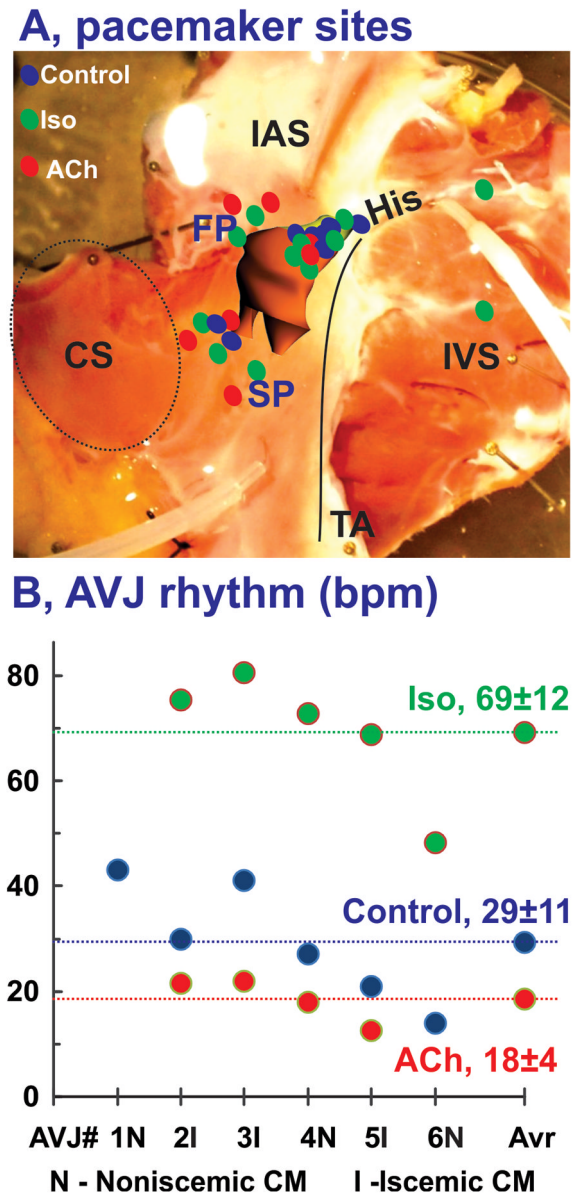

Figure 7.

Summary of anatomic locations of leading pacemaker sites in the human AVJ. **Panel A:** Summary of pacemaker sites identified in all hearts (n=6) in control (blue), under 1 μM Iso (green), and 1 μM ACh (red). **Panel B:** Individual for each heart and average (Avr) values for AVJ rhythm in control and during perfusion of Iso and ACh. CM- cardiomyopathy.

Table

Heart Failure Patient Histories.

Patient	Age	Gender	Diagnosis	Device	β-Blockers	Inotropes
1	52	Female	Nonischemic CM	AICD	No	No
2	55	Male	Ischemic CM	AICD	Yes	No
3	51	Male	Ischemic CM	LVAD	No	No
4	64	Male	Nonischemic CM	AICD	Yes	Yes
5	50	Male	Ischemic CM	BiV PPM/AICD	Yes	No
6	48	Male	Dilated CM		No	Yes

CM- cardiomyopathy; AICD –an implantable cardioverter defibrillator; LVAD – left ventricular assist device; BiV PPM – biventricular permanent pacemaker.